STRUCTURAL CHEMISTRY

Volume 79 (2023)

Supporting information for article:

Crystal structures, Hirshfeld analysis, and energy framework analysis of two differently 3′-substituted 4-methylchalcones: 3′-(N=CHC$_6$H$_4$-*p*-CH$_3$)-4-methylchalcone and 3′-(NHCOCH$_3$)-4-methylchalcone

Zachary O. Battaglia, Jordan T. Kersten, Elise M. Nicol, Paloma Whitworth, Kraig A. Wheeler, Charlie L. Hall, Jason Potticary, Victoria Hamilton, Simon R. Hall, Gemma D. D'Ambruoso, Masaomi Matsumoto, Stephen D. Warren and Matthew E. Cremeens

S1. Full Database Survey

A survey of the Cambridge Structural Database (CSD version 5.41, November 2019; Groom *et al.*, 2016), which excluded chalcones substituted with additional rings, revealed *m'*AA*p*CH_3 [Km6p] to be the first acetamido chalcone. No monosubstituted or disubstituted acetamido chalcone structures were found. One disubstituted chalcone had a substituent similar in structure to the acetamido group, a *p*$NHCO_2$-*t*-butyl on the 1-Ring, as well as a *p*-fluoro on the 3-Ring (YOKZEF; *P* 21/*n*; Mahawer *et al.*, 2013). Both YOKZEF and *m'*AA*p*CH_3 displayed a O1...HN1 contact, but this interaction contributed to an antiparallel stacking in *m'*AA*p*CH_3 and a linear arrangement in YOKZEF, and they differed in their space groups, *C*2/*c* and $P2_1$/n respectively. In order to expand the survey, additional chalcones that would display a similar hydrogen bonding interaction between the enone oxygen, and the 1-Ring substituent were included. A chalcone with a *m*-OH on the 1-Ring and a *p*CH_3 on the 3-Ring [Jm6p] (TIHQAD; $P2_1/n$; Butcher *et al.*, 2007) contained such an interaction, but did not also display the antiparallel stacking displayed in *m'*AA*p*CH_3; instead displaying a parallel stacking and differing in space group. Analysis of a chalcone with *o*-OH on the 1-Ring and *p*-CH_3 on the 3-Ring [Jo6p] (FAQFOS; *C*2/*c*; Shoja, 1999) showed more similarities, matching the space group of *m'*AA*p*CH_3 as well as its antiparallel stacking, but was missing the hydrogen bonding interaction formed between the 1-Ring substituent and the enone oxygen.

The same survey, this time excluding substituents without additional rings, again revealed no reported chalcones with a substituent matching the 1-Ring substituent on *m'*PM*p*CH_3 [Mm6p]. *m'*PM*p*CH_3, like *m'*AA*p*CH_3, is a unique, previously unreported chalcone. The survey was then expanded to include any chalcones with imino substituents, of which there were none, and finally to include any biphenyl substituents, of which there were multiple. One chalcone, 2-methyl-4'-phenylchalcone, [Tp6o] (XOFFEF; $P\bar{1}$; Shanthi *et al.*, 2014), contained both a biphenyl group and a methyl group, and another chalcone, 3-nitro-4'-phenylchalcone [Tp8m] (WOTRAA; *C*2/*c*; Shanthi *et al.*, 2015), contained a biphenyl and a nitro group. XOFFEF did not display any notable CH / π interactions based off the Hirshfeld analysis, unlike *m'*PM*p*CH_3, and did not match space groups with *m'*PM*p*CH_3. However, it did contain an interaction between the enone oxygen and the additional phenyl group; though in XOFFEF this interaction contributed to a parallel stacking arrangement, as opposed to this interaction giving rise to an antiparallel arrangement in *m'*PM*p*CH_3. WOTRAA matched space groups with *m'*PM*p*CH_3, both being *C*2/*c*, and both had strong interactions contributing to the antiparallel stacking of the crystal; enone carbonyl and additional phenyl for *m'*PM*p*CH_3, and enone carbonyl and enone hydrogen for WOTRAA. A difference arose when considering the role of CH / π interactions when it comes to stacking, with these interactions being between neighboring 3-Rings in *m'*PM*p*CH_3 and contributing to a parallel stacking structure, while the CH / π interaction of note in WOTRAA is between the 1-Ring and a neighboring phenyl substituent, also giving rise to a parallel structure. Note,

the Km6p, Mm6p, Jm6p Jo6p, Tp6o, and Tp8m codes presented here are internal codes tied to a larger long-term project.

S2. Hirshfeld Fingerprint Plots

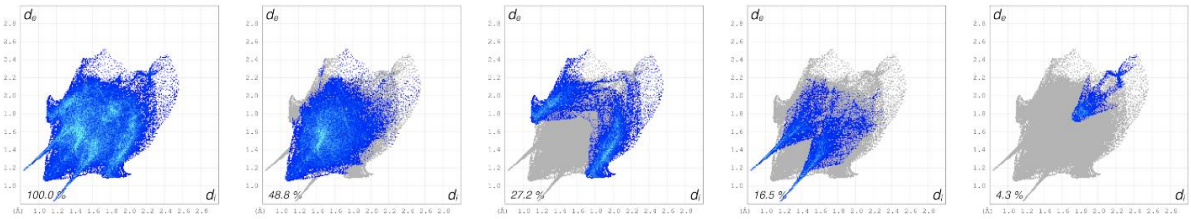

Figure S1 The two-dimensional fingerprint plots showing the percentage of contacts found by Hirshfeld surface analysis of *m*'AA*p*CH3.The contacts are shown from left to right: all, H···H (48.8%), H···C (27.2%), H···O (16.5%), and C···C (4.3%). These four contacts make up 96.8 % of the total contacts. No pictured are the fingerprint plots showing the less prominent H···N (1.0%), N···C (1.2%), and C···O (0.9%) contacts. For reference, the percentage contributions of the *m*'AA*p*CH_3 intermolecular contacts to the total Hirshfeld surface are: H···H (48.8%), C···H/H···C (27.2%), O···H/H···O (16.5%), N···H/H···N (1.0%), C···C (4.3%), O···C/C···O (0.9%), and C···N/N···C (1.2%). Note, the total is not 100%, but 99.9%.

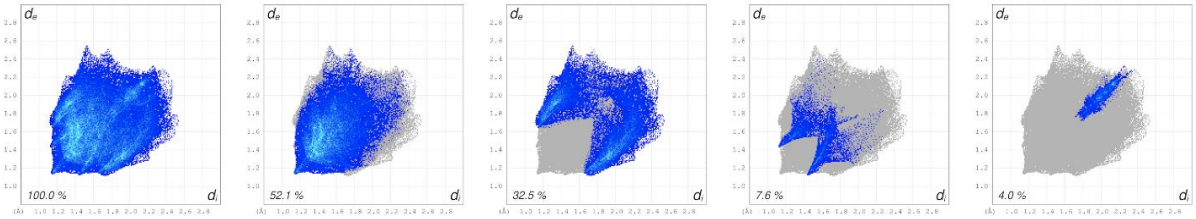

Figure S2 The two-dimensional fingerprint plots showing the percentage of contacts found by Hirshfeld surface analysis of *m*'PMI*p*CH_3. The contacts are shown from left to right: all, H···H (52.1%), H···C (32.5%), H···O (7.6%), and C···C (4.1%). These four contacts make up 96.3 % of the total contacts. Not pictured are the fingerprint plots showing the less prominent H···N (2.6%) and N···C (1.1%) contacts. For reference, the percentage contributions of the *m*'PMI*p*CH_3 intermolecular contacts to the total Hirshfeld surface are: H···H (52.1%), C···H/H···C (32.5%), O···H/H···O (7.6%), N···H/H···N (2.6%), C···C (4.1%), C···N/N···C (1.1%).

S3. Symmetry Operators

Table S1 *m*'PMI*p*CH3 and *m*'AA*p*CH_3 Symmetry Operators

#	Symm. Op.	Description	Detailed Description	Order	Type

1	x,y,z	Identity	Identity	1	1
2	-x,y,1/2-z	Rotation axis (2-fold)	2-fold rotation axis with direction [0, 1, 0] at 0, y, 1/4	2	2
3	1/2+x,1/2+y,z	Centring vector	Centring vector [1/2, 1/2, 0]	1	1
4	1/2-x,1/2+y,1/2-z	Screw axis (2-fold)	2-fold screw axis with direction [0, 1, 0] at 1/4, y, 1/4 with screw component [0, 1/2, 0]	2	2
5	-x,-y,-z	Inversion centre	Inversion at [0, 0, 0]	2	-1
6	x,-y,1/2+z	Glide plane	Glide plane perpendicular to [0, 1, 0] with glide component [0, 0, 1/2]	2	-2
7	1/2-x,1/2-y,-z	Inversion centre	Inversion at [1/4, 1/4, 0]	2	-1
8	1/2+x,1/2-y,1/2+z	Glide plane	Glide plane perpendicular to [0, 1, 0] with glide component [1/2, 0, 1/2]	2	-2

S4. Crystallization Details

Crystallization method for *m*'PMI*p*CH3 has been previously reported (Battaglia *et al.*, 2020). *m*'PMI*p*CH3 was crystallized through slow cooling in a hemispherical low form Dewar flask. Chalcone (20 mg), methanol (0.5 mL), and a magnetic spin vane were added to a conical Biotage microwave vial (0.5-2 mL) and sealed. The tube was submerged in boiling water for 1-5 minutes until complete dissolution. While the tube was submerged, two Dewar hemispherical low form flasks were filled with boiling water and allowed to sit. When chalcone was nearly dissolved, the Dewar flasks were emptied, and one was placed in a Styrofoam cooler. The Biotage microwave vial was removed from boiling water and placed in the Dewar inside the cooler. The Dewar was filled with boiling water to completely submerge the microwave vial. A round silicone gasket was placed to cover the rim of this Dewar flask before inverting the second Dewar and placing it on top to create a chamber. The cooler was closed with a Styrofoam lid on a low vibration table in a temperature regulated room. After 26-28 hours, the vials were removed from the Dewar and crystals were collected using vacuum filtration.

S5. Energy Framework Figures & Tables

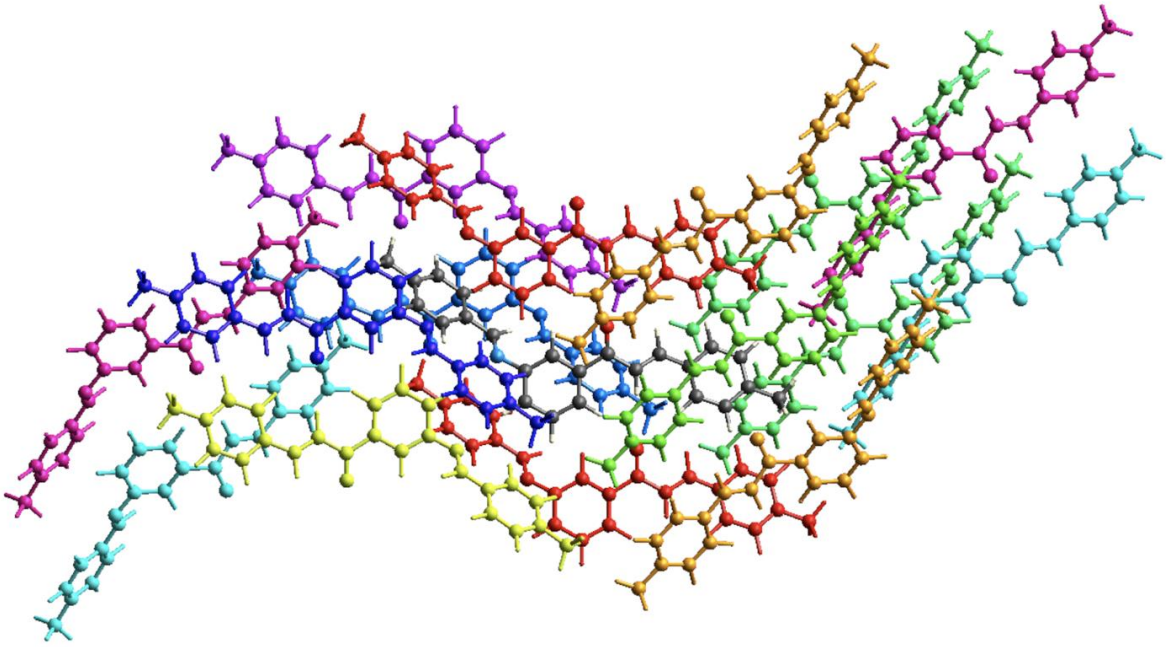

Figure S3 The interaction energies for a cluster of *m*′PMI*p*CH_3 molecules within a 3.8 Å radius of the central molecule colored in grey. The energies are color coded and correspond to SI Table S2.

Table S2 *Data Associated with SI Figure S3.* Interaction Energies (kJ/mol). R is the distance between molecular centroids (mean atomic position) in Å.

	N	Symop	R	Electron Density	E_ele	E_pol	E_dis	E_rep
	2	x, y, z	5.87	B3LYP/6-31G(d)	-18.9	-5.0	-66.8	47.1
	2	-x, y, -z+1/2	11.27	B3LYP/6-31G(d)	-1.9	-1.6	-15.4	6.9
	1	-x+1/2, -y+1/2, -z	10.51	B3LYP/6-31G(d)	-2.7	-0.9	-21.9	12.8
	1	-x, y, -z+1/2	9.62	B3LYP/6-31G(d)	-5.9	-2.4	-53.5	32.1
	2	-x+1/2, y+1/2, -z+1/2	14.68	B3LYP/6-31G(d)	-3.9	-0.5	-17.0	10.1
	2	x+1/2, -y+1/2, z+1/2	18.34	B3LYP/6-31G(d)	-1.2	-0.2	-8.7	5.3
	1	-x, -y, -z	6.41	B3LYP/6-31G(d)	-6.9	-1.6	-65.3	37.0
	1	-x+1/2, -y+1/2, -z	11.27	B3LYP/6-31G(d)	-8.7	-2.7	-38.1	26.8
	1	-x, -y, -z	9.60	B3LYP/6-31G(d)	-12.7	-5.5	-38.1	26.7
	2	x+1/2, -y+1/2, z+1/2	18.78	B3LYP/6-31G(d)	-0.2	-0.2	-6.1	3.4

Scale factors for benchmarked energy models. See Mackenzie *et al.* IUCrJ (2017).

Energy Model	k_ele	k_pol	k_disp	k_rep
CE-HF ... HF/3-21G electron densities	1.019	0.651	0.901	0.811
CE-B3LYP ... B3LYP/6-31G(d,p) electron densities	1.057	0.740	0.871	0.618

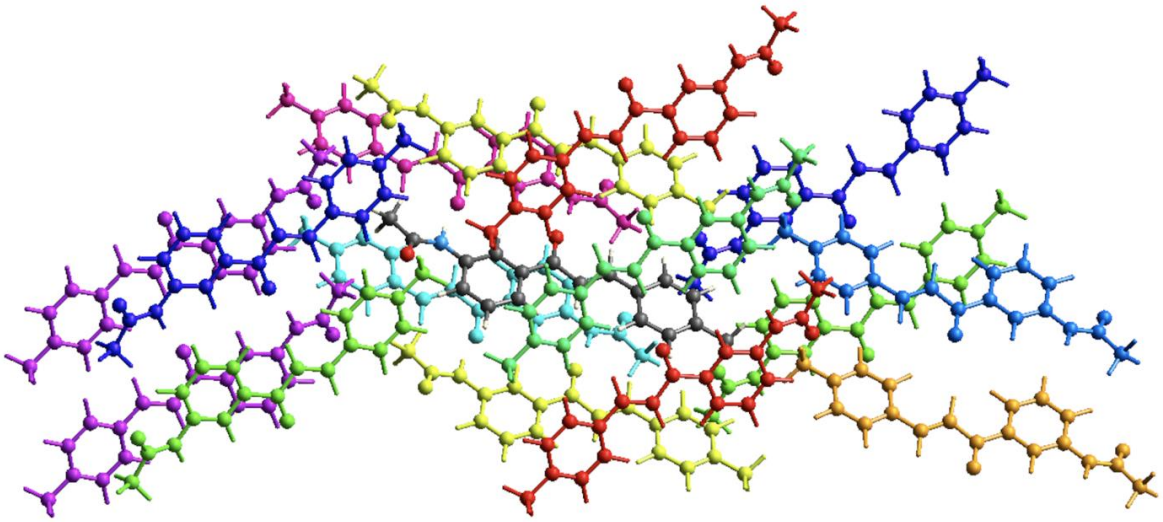

Figure S4 The interaction energies for a cluster of *m'*AA*p*CH_3 molecules within a 3.8 Å radius of the central molecule colored in grey. The energies are color coded and correspond to SI Table S3.

Table S3 *Data Associated with SI Figure S4.* Interaction Energies (kJ/mol)**.** R is the distance between molecular centroids (mean atomic position) in Å.

	N	Symop	R	E_ele	E_pol	E_dis	E_rep
	2	-x, y, -z+1/2	8.20	-4.3	-0.9	-20.8	11.0
	1	-x+1/2, -y+1/2, -z	19.35	-0.3	-0.1	-6.3	4.8
	2	x, y, z	5.76	-12.2	-3.6	-47.3	29.8
	2	x+1/2, -y+1/2, z+1/2	13.75	-5.9	-2.9	-11.4	11.7
	1	-x, y, -z+1/2	5.83	-8.0	-2.5	-54.7	38.2
	1	-x, -y, -z	4.57	-6.0	-4.1	-75.3	40.8
	1	-x+1/2, -y+1/2, -z	17.54	0.6	-0.2	-3.8	0.8
	2	x+1/2, -y+1/2, z+1/2	13.74	-7.1	-2.4	-11.0	8.9

	2	-x+1/2, y+1/2, -z+1/2	15.94	-3.9	-1.5	-6.8	4.8
	1	-x, -y, -z	7.35	-63.0	-16.6	-40.4	69.1

Scale factors for benchmarked energy models. See Mackenzie *et al.* IUCrJ (2017).

Energy Model	k_ele	k_pol	k_disp	k_rep
CE-HF ... HF/3-21G electron densities	1.019	0.651	0.901	0.811
CE-B3LYP ... B3LYP/6-31G(d,p) electron densities	1.057	0.740	0.871	0.618

Mackenzie, C. F., Spackman, P. R., Jayatilaka, D. & Mark A. Spackman, M. A. (2017). *IUCrJ*. **4**, 575-587.

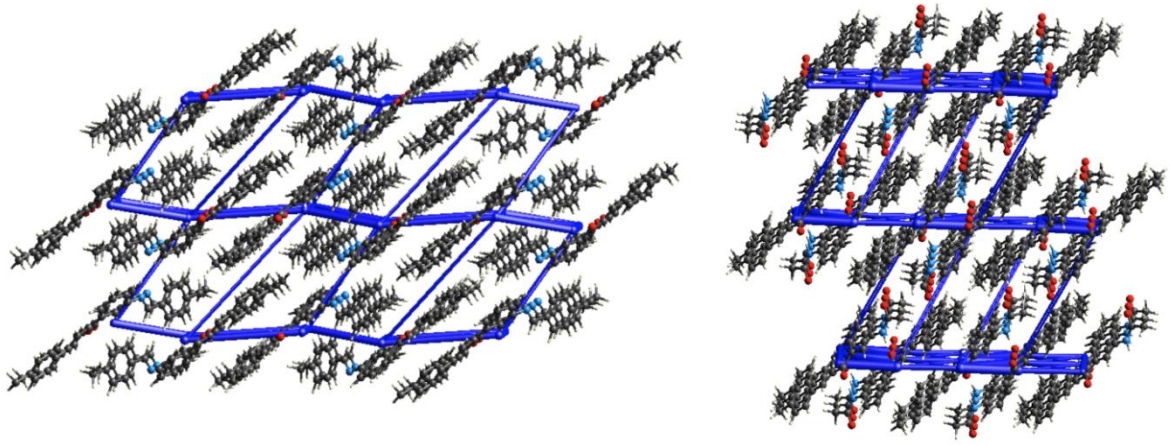

Figure S5 The total energy frameworks of *m'*PMI*p*CH_3 (left) and *m'*AA*p*CH_3 (right) looking down the *b* axis at the *a*/*c* face. The total energy frameworks are a representation of the sum of the scaled interaction energies shown in SI Figures 3 and 4. The energy frameworks are shown at the same scale factor of 90 with an energy cut-off value of 15 kJ mol^{-1} for 1 x 2 x 1 unit cells.

Table S4 Interaction energies were found from the total energy frameworks (SI Figure S5). The total energy for the *b*/*c* face of *m'*AA*p*CH_3 was calculated by taking the sum of the interaction energies between each molecule along the *b*/*c* face.

Interaction Energy (kJ/mol)	Multiple	Total Energy (kJ/mol)
-10	8	-80
-6.9	6	-41.4
-8.8	7	-61.6
-3	3	-9
-2.9	1	-2.9

		-194.9

Table S5 The area for the *b*/*c* face of *m'*AA*p*CH_3 was calculated by multiplying the distances between the centroids of the exterior molecules on each axis.

	Length (Å)
b-axis	5.792
c-axis	20.701
Area ($Å^2$)	119.3

Table S6 Interaction energies were found from the total energy frameworks (SI Figure S5). The total energy for the *b*/*c* face of *m'*PMI*p*CH_3 was calculated by taking the sum of the interaction energies between each molecule along the *b*/*c* face.

Interaction Energy (kJ/mol)	Multiple	Total Energy (kJ/mol)
-26.1	5	-130.5
-15.3	4	-61.2
-3.8	6	-22.8
-5.7	6	-34.2
-12.4	6	-74.4
		-323.1

Table S7 The area for the *b*/*c* face of *m'*PMI*p*CH_3 was calculated by multiplying the distances between the centroids of the exterior molecules on each axis.

	Length (Å)
b-axis	5.869
c-axis	31.371
Area ($Å^2$)	184.1

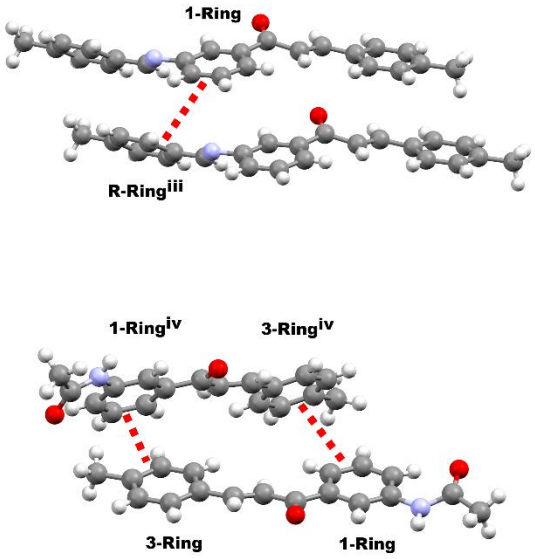

Figure S6 Π-stacking interactions shown between the 1-Ring/ R-Ring of *m'*PMI*p*CH_3 (top) and the 1-Ring/ 3 Ring of *m'*AA*p*CH_3 (bottom). The symmetry codes apply to those molecules interacting with the asymmetric unit. Symmetry Codes *m'*PMI*p*CH_3: (i) *1-x, 2-y, 1-z;* (ii) *1-x, +y, 3/2-z*; (iii) *+x, -1+y, +z*. *m'*AA*p*CH_3: (i) *1-x, 2-y, 1-z*; (ii) *1/2+x, 1/2-y, 1/2+z*; (iii) *1/2+x, 3/2-y, 1/2+z*; (iv) *1-x, +y, ½-z*.

S6. NMR Spectra

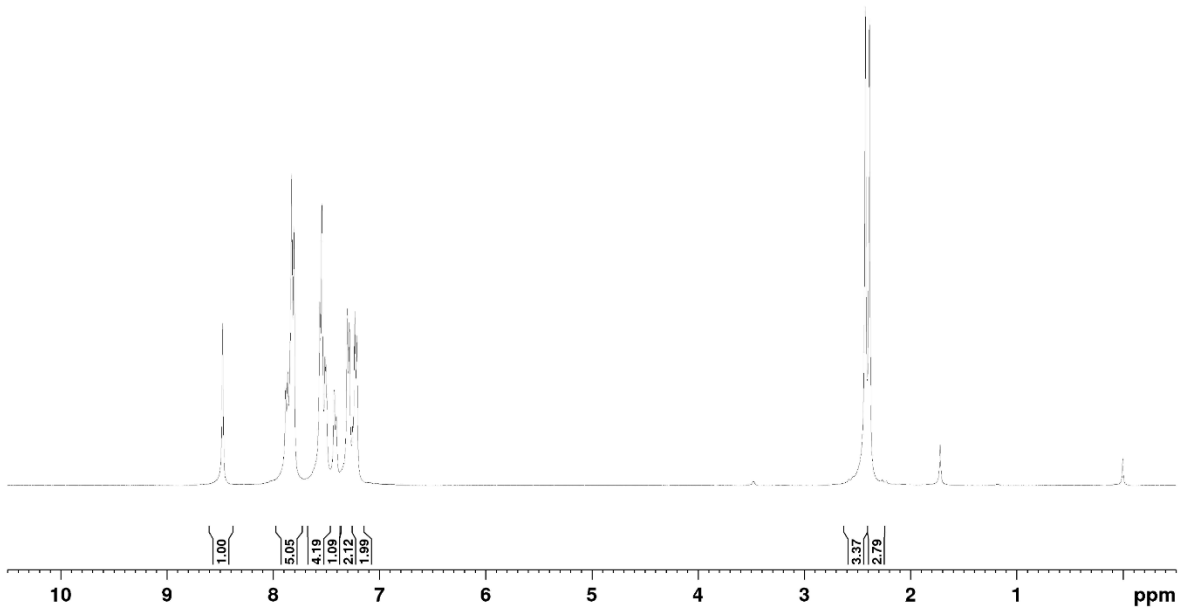

Figure S7 ^{1}H NMR of *m'*PMI*p*CH_3 (Mm6p)

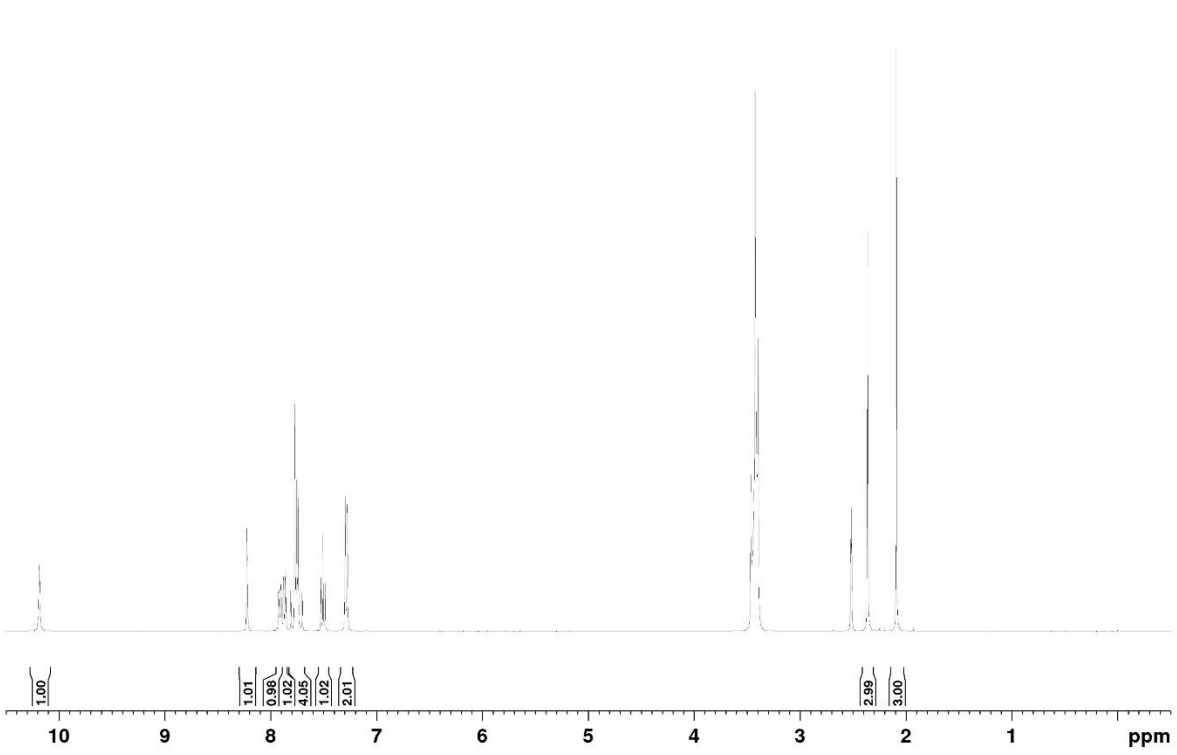

Figure S8 ^{1}H NMR of *m'*AA*p*CH$_3$ (Km6p)

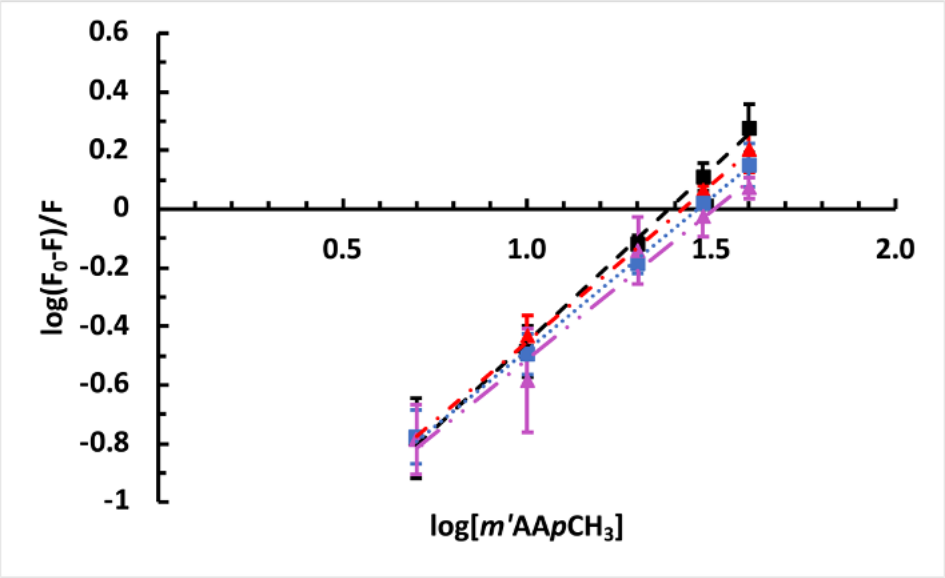

Figure S9 **Binding constant *m'*AA*p*CH$_3$.** Plot for log(F$_0$-F)/F versus log[*m'*AA*p*CH$_3$] with linear equation of best fit. The y intercept is equal to log(*K*), where *K* is the binding constant. The slope is equal to *n*, where *n* is the number of binding sites. The standard deviation for the three trials is

represented by error bars. Black square (dash-dash): 298 K (25 °C); Red triangle (dash-dot): 303 K (30 °C); Blue square (dot-dot): 308 K (35 °C); Magenta triangle (dash-dot-dot): 313 K (40 °C).

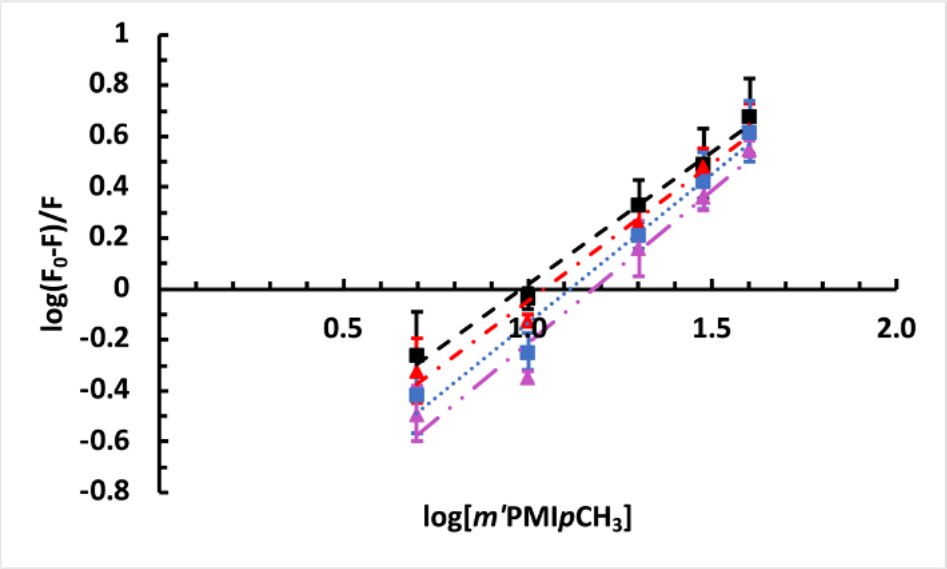

Figure S10 Binding constant *m*'PMI*p*CH$_3$. Plot for log(F_0-F)/F versus log[*m*'AA*p*CH_3] with linear equation of best fit. The y intercept is equal to log(*K*), where *K* is the binding constant. The slope is equal to *n*, where *n* is the number of binding sites. The standard deviation for the three trials is represented by error bars. Black square (dash-dash): 298 K (25 °C); Red triangle (dash-dot): 303 K (30 °C); Blue square (dot-dot): 308 K (35 °C); Magenta triangle (dash-dot-dot): 313 K (40 °C)

Table S8 Binding constants (*K*) and the number of binding sites (*n*) for *m*'AA*p*CH_3 at temperatures ranging from 298 K (25 °C) to 313 K (40 °C). These values were calculated from the linear equations of best fit from lines in figure 10 and equation 3.

T (K / °C)	K^a (x 10^4 L mol^{-1})	n^b	R^c
298 / 25	2.3 ± 0.2	1.18	0.996
303 / 30	3.1 ± 0.2	1.07	0.997
308 / 35	3.1 ± 0.6	1.03	0.998
313 / 40	3.0 ± 0.6	1.01	0.980

[a]The binding constant

[b]The number of binding sites per protein

[c]The correlation coefficient

Table S9 Binding constants (*K*) and the number of binding sites (*n*) for *m*'PMI*p*CH_3 at temperatures ranging from 298 K (25 °C) to 313 K (40 °C). These values were calculated from the linear equations of best fit from lines in figure 12 and equation 3.

T (K / °C)	K^a (x 10^4 L mol^{-1})	n^b	R^c

298 / 25	9 ± 1	1.04	0.990
303 / 30	5 ± 1	1.08	0.985
308 / 35	5 ± 1	1.18	0.974
313 / 40	4 ± 1	1.20	0.968

[a]The binding constant

[b]The number of binding sites per protein

[c]The correlation coefficient

S7. Computing details

Data collection: *APEX3* v2018.7-2 (Bruker, 2020); cell refinement: *SAINT* V8.38A (Bruker, 2020); data reduction: *SAINT* V8.38A (Bruker, 2017); program(s) used to solve structure: SHELXT-2018/2 (Sheldrick, 2015a); program(s) used to refine structure: *SHELXL2018*/3 (Sheldrick, 2015b); molecular graphics: *X-SEED* (Barbour, 2001); software used to prepare material for publication: *X-SEED* (Barbour, 2001).

*S8. Crystal data m'***AA***p***CH$_3$** **(*Km6p, CCDC Deposition #: 2029928)***

$C_{18}H_{17}NO_2$	$F(000)$ = 1184
M_r = 279.32	D_x = 1.306 Mg m^{-3}
Monoclinic, *C*2/*c*	Cu *K*α radiation, λ = 1.54178 Å
a = 25.1922 (5) Å	Cell parameters from 9920 reflections
b = 5.7621 (1) Å	θ = 3.7–72.1°
c = 20.7012 (4) Å	μ = 0.68 mm^{-1}
β = 109.066 (1)°	*T* = 100 K
V = 2840.14 (9) Å^3	Prism, colourless
Z = 8	0.46 × 0.17 × 0.15 mm

Data collection

Bruker D8 Venture diffractometer	2786 independent reflections
Radiation source: Microsource IuS Incoatec 3.0	2596 reflections with $I > 2\sigma(I)$
Double Bounce Multilayer Mirrors monochromator	R_{int} = 0.025
Detector resolution: 7.9 pixels mm^{-1}	θ_{max} = 72.2°, θ_{min} = 3.7°
ϕ and ω scans	*h* = -30→30
Absorption correction: multi-scan SADABS2016/2 (Bruker AXS)	*k* = -7→6
T_{min} = 0.646, T_{max} = 0.754	*l* = -25→25
14321 measured reflections	

Refinement

Refinement on F^2	Primary atom site location: structure-invariant direct methods
Least-squares matrix: full	Hydrogen site location: mixed
$R[F^2 > 2\sigma(F^2)] = 0.034$	H atoms treated by a mixture of independent and constrained refinement
$wR(F^2) = 0.091$	$w = 1/[\sigma^2(F_o^2) + (0.0459P)^2 + 2.0674P]$ where $P = (F_o^2 + 2F_c^2)/3$
$S = 1.05$	$(\Delta/\sigma)_{max} = 0.001$
2786 reflections	$\Delta\rangle_{max} = 0.24$ e Å^{-3}
195 parameters	$\Delta\rangle_{min} = -0.18$ e Å^{-3}
0 restraints	

Special details

Geometry. All esds (except the esd in the dihedral angle between two l.s. planes) are estimated using the full covariance matrix. The cell esds are taken into account individually in the estimation of esds in distances, angles and torsion angles; correlations between esds in cell parameters are only used when they are defined by crystal symmetry. An approximate (isotropic) treatment of cell esds is used for estimating esds involving l.s. planes.
Refinement. All nonhydrogen atoms were located in a single difference Fourier electron density map and refined using anisotropic displacement parameters. All C—H hydrogen atoms were placed in calculated positions with Uiso = 1.2xUeqiv of the connected C atoms (1.5xUeqiv for methyl groups). The H atom attached to nitro-gen N1 was located in Fourier diff map and assigned Uiso = 1.5xUeqiv.

Fractional atomic coordinates and isotropic or equivalent isotropic displacement parameters (Å^2) for (cu_20mec13)

	x	*y*	*z*	U_{iso}*/U_{eq}
O1	0.46820 (3)	0.81616 (14)	0.39168 (4)	0.0250 (2)
O2	0.72479 (3)	0.81750 (17)	0.64907 (4)	0.0312 (2)
N1	0.63056 (4)	0.88412 (16)	0.60966 (4)	0.0186 (2)
HN1	0.6047 (6)	0.979 (3)	0.6119 (7)	0.028*
C1	0.49200 (4)	0.62787 (19)	0.39523 (5)	0.0186 (2)
C2	0.46888 (4)	0.4432 (2)	0.34406 (5)	0.0206 (2)
H2	0.485316	0.293005	0.351190	0.025*
C3	0.42525 (4)	0.4852 (2)	0.28807 (5)	0.0197 (2)
H3	0.410823	0.638878	0.283304	0.024*
C4	0.54573 (4)	0.58199 (19)	0.45210 (5)	0.0172 (2)
C5	0.56419 (4)	0.74641 (19)	0.50440 (5)	0.0172 (2)
H5	0.542254	0.881225	0.503505	0.021*
C6	0.61438 (4)	0.71465 (19)	0.55778 (5)	0.0166 (2)
C7	0.64652 (4)	0.51542 (19)	0.55888 (5)	0.0188 (2)
H7	0.680734	0.491344	0.595127	0.023*
C8	0.62815 (5)	0.3539 (2)	0.50687 (6)	0.0212 (2)
H8	0.650112	0.219210	0.507728	0.025*
C9	0.57818 (4)	0.38495 (19)	0.45336 (5)	0.0199 (2)
H9	0.566228	0.272749	0.417922	0.024*
C10	0.39684 (4)	0.32381 (19)	0.23303 (5)	0.0181 (2)
C11	0.34430 (5)	0.38547 (19)	0.18694 (5)	0.0204 (2)
H15	0.327915	0.529786	0.192141	0.025*
C12	0.31589 (4)	0.2384 (2)	0.13378 (5)	0.0202 (2)
H14	0.279916	0.282282	0.103821	0.024*
C13	0.33906 (4)	0.02806 (19)	0.12351 (5)	0.0191 (2)
C14	0.39167 (4)	-0.03316 (19)	0.16940 (5)	0.0200 (2)
H12	0.408461	-0.175418	0.163221	0.024*

C15	0.41973 (4)	0.10988 (19)	0.22367 (5)	0.0193 (2)
H11	0.454871	0.062276	0.254867	0.023*
C16	0.68404 (4)	0.9267 (2)	0.65190 (5)	0.0192 (2)
C17	0.68940 (5)	1.1167 (2)	0.70315 (6)	0.0231 (3)
H17A	0.682174	1.053758	0.743465	0.035*
H17B	0.662072	1.239254	0.682788	0.035*
H17C	0.727444	1.181337	0.716695	0.035*
C18	0.30808 (5)	-0.1296 (2)	0.06553 (6)	0.0238 (3)
H18A	0.281767	-0.226556	0.079507	0.036*
H18B	0.335026	-0.228993	0.053528	0.036*
H18C	0.287275	-0.036090	0.025790	0.036*

Atomic displacement parameters (Å^2) for (cu_20mec13)

	U^{11}	U^{22}	U^{33}	U^{12}	U^{13}	U^{23}
O1	0.0218 (4)	0.0224 (4)	0.0252 (4)	0.0049 (3)	0.0002 (3)	-0.0060 (3)
O2	0.0169 (4)	0.0408 (5)	0.0333 (5)	0.0008 (4)	0.0047 (3)	-0.0127 (4)
N1	0.0164 (4)	0.0197 (5)	0.0187 (4)	0.0018 (4)	0.0043 (3)	-0.0025 (4)
C1	0.0178 (5)	0.0196 (5)	0.0190 (5)	-0.0002 (4)	0.0068 (4)	-0.0017 (4)
C2	0.0203 (5)	0.0182 (5)	0.0216 (5)	0.0006 (4)	0.0046 (4)	-0.0033 (4)
C3	0.0202 (5)	0.0179 (5)	0.0210 (5)	-0.0010 (4)	0.0066 (4)	-0.0019 (4)
C4	0.0167 (5)	0.0191 (5)	0.0168 (5)	-0.0012 (4)	0.0066 (4)	-0.0005 (4)
C5	0.0165 (5)	0.0168 (5)	0.0190 (5)	0.0015 (4)	0.0068 (4)	0.0000 (4)
C6	0.0171 (5)	0.0182 (5)	0.0159 (5)	-0.0023 (4)	0.0072 (4)	-0.0005 (4)
C7	0.0175 (5)	0.0210 (5)	0.0169 (5)	0.0019 (4)	0.0045 (4)	0.0032 (4)
C8	0.0225 (5)	0.0188 (5)	0.0228 (5)	0.0052 (4)	0.0080 (4)	0.0009 (4)
C9	0.0221 (5)	0.0196 (5)	0.0180 (5)	0.0007 (4)	0.0066 (4)	-0.0026 (4)
C10	0.0180 (5)	0.0192 (5)	0.0171 (5)	-0.0033 (4)	0.0057 (4)	-0.0013 (4)
C11	0.0218 (5)	0.0185 (5)	0.0208 (5)	0.0007 (4)	0.0068 (4)	-0.0001 (4)
C12	0.0182 (5)	0.0233 (6)	0.0173 (5)	-0.0027 (4)	0.0035 (4)	0.0005 (4)
C13	0.0218 (5)	0.0211 (6)	0.0167 (5)	-0.0073 (4)	0.0093 (4)	-0.0016 (4)
C14	0.0216 (5)	0.0185 (5)	0.0224 (5)	-0.0017 (4)	0.0107 (4)	-0.0022 (4)
C15	0.0162 (5)	0.0210 (6)	0.0204 (5)	-0.0007 (4)	0.0058 (4)	0.0000 (4)
C16	0.0174 (5)	0.0235 (5)	0.0160 (5)	-0.0025 (4)	0.0046 (4)	0.0008 (4)
C17	0.0207 (5)	0.0269 (6)	0.0204 (5)	-0.0031 (4)	0.0049 (4)	-0.0034 (4)
C18	0.0270 (6)	0.0259 (6)	0.0192 (5)	-0.0082 (5)	0.0084 (4)	-0.0051 (4)

Geometric parameters (Å, º) for (cu_20mec13)

O1—C1	1.2302 (14)	C9—H9	0.9500
O2—C16	1.2219 (14)	C10—C15	1.4010 (15)
N1—C16	1.3675 (13)	C10—C11	1.4011 (15)
N1—C6	1.4097 (14)	C11—C12	1.3880 (15)
N1—HN1	0.862 (16)	C11—H15	0.9500
C1—C2	1.4800 (15)	C12—C13	1.3917 (16)
C1—C4	1.4989 (14)	C12—H14	0.9500
C2—C3	1.3333 (15)	C13—C14	1.4003 (15)
C2—H2	0.9500	C13—C18	1.5044 (15)
C3—C10	1.4638 (14)	C14—C15	1.3865 (15)
C3—H3	0.9500	C14—H12	0.9500
C4—C9	1.3943 (15)	C15—H11	0.9500
C4—C5	1.3990 (15)	C16—C17	1.4997 (15)
C5—C6	1.3930 (14)	C17—H17A	0.9800
C5—H5	0.9500	C17—H17B	0.9800
C6—C7	1.4007 (15)	C17—H17C	0.9800
C7—C8	1.3835 (16)	C18—H18A	0.9800

C7—H7	0.9500	C18—H18B	0.9800
C8—C9	1.3903 (15)	C18—H18C	0.9800
C8—H8	0.9500		
C16—N1—C6	126.20 (9)	C11—C10—C3	118.81 (10)
C16—N1—HN1	117.2 (10)	C12—C11—C10	120.86 (10)
C6—N1—HN1	116.3 (10)	C12—C11—H15	119.6
O1—C1—C2	121.41 (10)	C10—C11—H15	119.6
O1—C1—C4	119.99 (10)	C11—C12—C13	121.29 (10)
C2—C1—C4	118.60 (9)	C11—C12—H14	119.4
C3—C2—C1	120.78 (10)	C13—C12—H14	119.4
C3—C2—H2	119.6	C12—C13—C14	117.85 (10)
C1—C2—H2	119.6	C12—C13—C18	120.92 (10)
C2—C3—C10	128.03 (11)	C14—C13—C18	121.23 (10)
C2—C3—H3	116.0	C15—C14—C13	121.26 (10)
C10—C3—H3	116.0	C15—C14—H12	119.4
C9—C4—C5	119.49 (10)	C13—C14—H12	119.4
C9—C4—C1	122.13 (10)	C14—C15—C10	120.74 (10)
C5—C4—C1	118.37 (9)	C14—C15—H11	119.6
C6—C5—C4	120.74 (10)	C10—C15—H11	119.6
C6—C5—H5	119.6	O2—C16—N1	123.00 (10)
C4—C5—H5	119.6	O2—C16—C17	121.81 (10)
C5—C6—C7	119.39 (10)	N1—C16—C17	115.19 (9)
C5—C6—N1	118.36 (9)	C16—C17—H17A	109.5
C7—C6—N1	122.25 (9)	C16—C17—H17B	109.5
C8—C7—C6	119.60 (9)	H17A—C17—H17B	109.5
C8—C7—H7	120.2	C16—C17—H17C	109.5
C6—C7—H7	120.2	H17A—C17—H17C	109.5
C7—C8—C9	121.28 (10)	H17B—C17—H17C	109.5
C7—C8—H8	119.4	C13—C18—H18A	109.5
C9—C8—H8	119.4	C13—C18—H18B	109.5
C8—C9—C4	119.50 (10)	H18A—C18—H18B	109.5
C8—C9—H9	120.2	C13—C18—H18C	109.5
C4—C9—H9	120.2	H18A—C18—H18C	109.5
C15—C10—C11	117.97 (10)	H18B—C18—H18C	109.5
C15—C10—C3	123.22 (10)		
O1—C1—C2—C3	8.13 (16)	C5—C4—C9—C8	0.53 (16)
C4—C1—C2—C3	-171.62 (10)	C1—C4—C9—C8	178.84 (10)
C1—C2—C3—C10	-179.22 (10)	C2—C3—C10—C15	-14.93 (17)
O1—C1—C4—C9	-171.19 (10)	C2—C3—C10—C11	165.48 (11)
C2—C1—C4—C9	8.57 (15)	C15—C10—C11—C12	0.12 (15)
O1—C1—C4—C5	7.14 (15)	C3—C10—C11—C12	179.73 (10)
C2—C1—C4—C5	-173.11 (9)	C10—C11—C12—C13	-1.50 (16)
C9—C4—C5—C6	-0.36 (15)	C11—C12—C13—C14	1.20 (15)
C1—C4—C5—C6	-178.73 (9)	C11—C12—C13—C18	-179.68 (10)
C4—C5—C6—C7	-0.07 (15)	C12—C13—C14—C15	0.46 (15)
C4—C5—C6—N1	-179.07 (9)	C18—C13—C14—C15	-178.65 (9)

C16—N1—C6—C5	-156.74 (10)	C13—C14—C15—C10	-1.84 (16)
C16—N1—C6—C7	24.29 (16)	C11—C10—C15—C14	1.52 (15)
C5—C6—C7—C8	0.33 (15)	C3—C10—C15—C14	-178.07 (10)
N1—C6—C7—C8	179.29 (9)	C6—N1—C16—O2	-0.32 (17)
C6—C7—C8—C9	-0.16 (16)	C6—N1—C16—C17	-179.59 (10)
C7—C8—C9—C4	-0.28 (16)		

Hydrogen-bond geometry (Å, º) for (cu_20mec13)

D—H···*A*	*D*—H	H···*A*	*D*···*A*	*D*—H···*A*
N1—H*N*1···O1^{i}	0.862 (16)	2.165 (16)	3.0213 (12)	172.3 (14)
C7—H7···O2	0.95	2.28	2.8281 (14)	116

Symmetry code: (i) -*x*+1, -*y*+2, -*z*+1.

Document origin: *publCIF* [Westrip, S. P. (2010). *J. Apply. Cryst.*, **43**, 920-925].